J Neurophysiol 109: 2382–2392, 2013.
First published February 6, 2013; doi:10.1152/jn.00430.2012.

Voltage-sensitive dye imaging reveals shifting spatiotemporal spread of whisker-induced activity in rat barrel cortex

Brian R. Lustig, Robert M. Friedman, Jeremy E. Winberry, Ford F. Ebner, and Anna W. Roe
Department of Psychology, Vanderbilt University, Nashville, Tennessee

Submitted 22 May 2012; accepted in final form 6 February 2013

Lustig BR, Friedman RM, Winberry JE, Ebner FF, Roe AW. Voltage-sensitive dye imaging reveals shifting spatiotemporal spread of whisker-induced activity in rat barrel cortex. *J Neurophysiol* 109: 2382–2392, 2013. First published February 6, 2013; doi:10.1152/jn.00430.2012.—In rats, navigating through an environment requires continuous information about objects near the head. Sensory information such as object location and surface texture are encoded by spike firing patterns of single neurons within rat barrel cortex. Although there are many studies using single-unit electrophysiology, much less is known regarding the spatiotemporal pattern of activity of populations of neurons in barrel cortex in response to whisker stimulation. To examine cortical response at the population level, we used voltage-sensitive dye (VSD) imaging to examine ensemble spatiotemporal dynamics of barrel cortex in response to stimulation of single or two adjacent whiskers in urethane-anesthetized rats. Single whisker stimulation produced a poststimulus fluorescence response peak within 12–16 ms in the barrel corresponding to the stimulated whisker (principal whisker). This fluorescence subsequently propagated throughout the barrel field, spreading anisotropically preferentially along a barrel row. After paired whisker stimulation, the VSD signal showed sublinear summation (less than the sum of 2 single whisker stimulations), consistent with previous electrophysiological and imaging studies. Surprisingly, we observed a spatial shift in the center of activation occurring over a 10- to 20-ms period with shift magnitudes of 1–2 barrels. This shift occurred predominantly in the posteromedial direction within the barrel field. Our data thus reveal previously unreported spatiotemporal patterns of barrel cortex activation. We suggest that this nontopographical shift is consistent with known functional and anatomic asymmetries in barrel cortex and that it may provide an important insight for understanding barrel field activation during whisking behavior.

whisker function; optical imaging; somatosensory; barrel cortex; VSD

IN RODENTS, THE TOPOGRAPHICAL single whisker-to-single cortical barrel relationship has long been recognized as a principle of cortical functional organization (Woolsey and Van der Loos 1970). Despite this clear one-to-one relationship, neurophysiological studies have revealed that principal whiskers are also modulated by subthreshold influences from distant sites (Brecht and Sakmann 2002; Ghazanfar and Nicolelis 1999; Higley and Contreras 2003, 2005; Manns et al. 2004; Moore and Nelson 1998; Veinante and Deschenes 1999). For example, anisotropic suppressive effects of an adjacent whisker on principal whisker neuron response have been demonstrated (Simons 1983, 1985; Simons and Carvell 1989), suggesting that there may be spatial asymmetries in inhibitory interactions across the barrel field (cf. McCasland et al. 1991). In addition to spatial interaction effects, there are also temporal dependencies (Armstrong-James and Fox 1987; Simons 1985). Displacing whiskers with different interwhisker stimulation times (from 0 to 40 ms) produces either suppression or facilitation of primary whisker responses depending on the interstimulus interval (Bruno and Simons 2002; Shimegi et al. 1999, 2000; Simons and Carvell 1983, 1989). These results suggest the response of cortical barrel field is a result of a complex array of spatial and temporal interactions. Although electrophysiological studies have given us tremendous understanding of single-neuron behavior in barrel cortex, we lack a good understanding of the spatiotemporal profile of the population response across the whisker barrel field, something that is extremely relevant for understanding cortical activity during whisking behavior in rodents that actively move their whiskers.

To examine the population response of barrel cortex in rats, we have used the voltage-sensitive dye (VSD) imaging method to provide high spatial and temporal resolution visualization of cortical activity. VSD imaging measures changes in membrane potential over large populations of neurons primarily in layer 2/3 of cortex (Civillico and Contreras 2006; Ferezou et al. 2006; Jin et al. 2002; Kleinfeld and Delaney 1996; Lippert et al. 2007) and is thus useful for revealing the time and spread of barrel responses as well as more distant subthreshold modulatory response. Civillico and Contreras (2006) used this method to study barrel fields in mice and found, surprisingly, only suppressive effects in multiwhisker responses. There are several differences between barrel field of the mouse and rat species, including distinctly different arrangements on the level of cytoarchitecture and overall laminar connectivity (Bureau et al. 2006; Simons and Woolsey 1984; Welker and Woolsey 1974). Unlike mice, rats have more developed septal zones (Petersen and Sakmann 2001), regions that are not dominated by a single principal whisker but respond equally well to two or three whiskers (Alloway 2008; Kim and Ebner 1999). This raises the possibility of differences in spatiotemporal activation profiles between these two species. Whether multiwhisker stimulation in the rat leads to facilitation or suppression at the population level remains unclear (although see Kleinfeld and Delaney 1996 for alternating multiwhisker stimulation in rats).

In this study, we examined the cortical response to single and paired whisker stimulation with VSD methods. Our results show that paired whisker stimulation leads to sublinear summation of responses compared with single whisker stimulation. In addition, over a 10- to 20-ms period following whisker stimulation, we found a surprising nontopographical shift in activation over a distance of one to three barrels away from the center of the initially stimulated whisker barrel.

MATERIALS AND METHODS

Surgical procedures. Four adult Long-Evans rats weighing 250–450 g were used for VSD imaging. All procedures were conducted in accordance with National Institutes of Health guidelines and were approved by the Vanderbilt University Animal Care and Use Com-

Address for reprint requests and other correspondence: A. W. Roe, Dept. of Psychology, Vanderbilt Univ., 301 Wilson Hall, 111 21st Ave. South, Nashville, TN 37203 (e-mail: anna.roe@vanderbilt.edu).

mittee. Rats were anesthetized with urethane [1.5 g/kg, 30% aqueous solution, intraperitoneally (IP)] and given additional doses as needed to maintain surgical levels of anesthesia. After initial sedation, rats were given 0.03 mg/kg atropine sulfate by intramuscular injection as well as 1 ml of lactated Ringer IP. A tracheotomy was performed and the animal ventilated. A craniotomy was carefully performed over the left hemisphere centered over barrel cortex, with 0.2-g mannitol injected IP just before removal of the skull as a preventative measure to minimize brain swelling. Dura was then carefully removed. Cortex was covered with 4% agar and a glass coverslip to reduce pulsation and to create an optical window.

Optical imaging. A charge-coupled device (CCD) camera (NeuroCCD 256; SciMeasure Analytical Systems, Decatur, GA) was positioned over the craniotomy. Images were collected with a Redshirt Imaging System running CortiPlex software (Redshirt Imaging, Decatur, GA). Initially, intrinsic optical imaging (632-nm illumination) was performed by using previously published methods (Cayce et al. 2011) to functionally locate barrel cortex. To localize the barrels, several rostral (*condition 1*) or caudal whiskers (*condition 2*) were stimulated and the activation maps were compared with a blank no-stimulus condition (*condition 3*). The imaging run consisted of 20–50 trials of each stimulus condition. Trial averaging was used to improve signal-to-noise ratio.

Subsequently, barrel cortex was stained with the VSD RH-1691 or RH-1692 (Optical Imaging, New York, NY) dissolved in artificial cerebrospinal fluid by applying, for 1.5–2 h, dye to cortex exposed by excising the covering agar. After staining, cortex was again covered with 4% agar and a glass coverslip. For VSD imaging, cortical exposure to 632-nm illumination was gated by an externally controlled shutter (Uniblitz; Vincent Associates, Rochester, NY) to minimize light exposure and dye bleaching. To image VSD fluorescence, the camera lens was outfitted with a 650-nm high-pass filter. The CCD camera acquired frames at either 100 Hz with a 256 × 256-pixel array or 360 Hz with a 64 × 64-pixel array.

All whiskers were trimmed on the contralateral whisker pad except for C2, C3, and C4. Individual piezoceramic actuators (Noliac, Alpharetta, GA) were arranged to contact the whiskers 5 mm from each whisker base. Each piezoceramic stimulator was driven by a 20-ms 75-V square-wave pulse (S88 stimulator; Astro-Med, West Warwick, RI) calibrated to displace each whisker ~250–300 μm in a rostral direction equal to a peak velocity of ~1,700°/s. For each imaging trial, an in-house written computer program (LabVIEW; National Instruments, Austin, TX) controlled the temporal sequence of events. The sequence was as follows: *1*) each trial began with illumination shutter opening at 100 ms before whisker stimulation and illumination of cortex with 632-nm light; *2*) the CCD camera started acquiring frames 80 ms before whisker stimulation; *3*) at 0 ms, whiskers were stimulated for 20 ms; *4*) at 180 ms, the camera stopped collecting frames and the shutter was closed, blocking the 632-nm illumination; and *5*) an 8-s interstimulus interval separated trials.

To explore multiwhisker interactions, we compared maps generated by four to six conditions. The conditions included *1*) C2 stimulation, *2*) C3 stimulation, *3*) C4 stimulation, *4*) simultaneous C2 and C3 stimulation, *5*) simultaneous C3 and C4 stimulation, and *6*) no whisker stimulation. Each imaging run consisted of 50–100 trials of each stimulus condition in random order.

Image analysis. Multiple steps of image analysis were used to measure the spatial and temporal spread of neural activity (fluorescence) in barrel field cortex. Image analysis consisted of *1*) aligning the field of view (FOV) of the image maps with the underlying anatomy, *2*) generating functional maps within the image frames, and *3*) selecting a region of interest (ROI) for time course signal analysis.

Image alignment with anatomy and ROI selection. To select ROIs for image analysis as well as to link the anatomic with the functional aspects of the images, a cortical blood vessel map of the camera's FOV was acquired with green light (578 nm). The FOV was 4 × 4 mm for the collected images (Fig. 1*A*).

After an imaging session, the brain was perfused with 4% paraformaldehyde in PBS and 40-μm frozen sections were cut parallel to the pial surface (tangential plane) and stained for cytochrome oxidase activity (Wong-Riley 1979). The blood vessel image was aligned with the vessel patterns in the most superficial sections to register the FOV with the histology (Fig. 1*B*) and the cytochrome oxidase-stained barrels in layer IV (Fig. 1*C*). The boundaries of the cytochrome-defined whisker cortical barrels (Fig. 1*D*) were then superimposed over the optical images (Fig. 1, *E* and *F*).

Image processing. To generate maps for visualizing the spread of activity and for making threshold measurements of the area of activation, the raw fluorescence (ΔF/F) images (Fig. 1*F*) were spatially filtered using a spatial Gaussian filter with a sigma of 2.00 pixels for the 360-Hz images (64 × 64 pixels) and a sigma of 8.00 pixels for 100-Hz images (256 × 256 pixels) (Fig. 1*G*). With the map of barrel

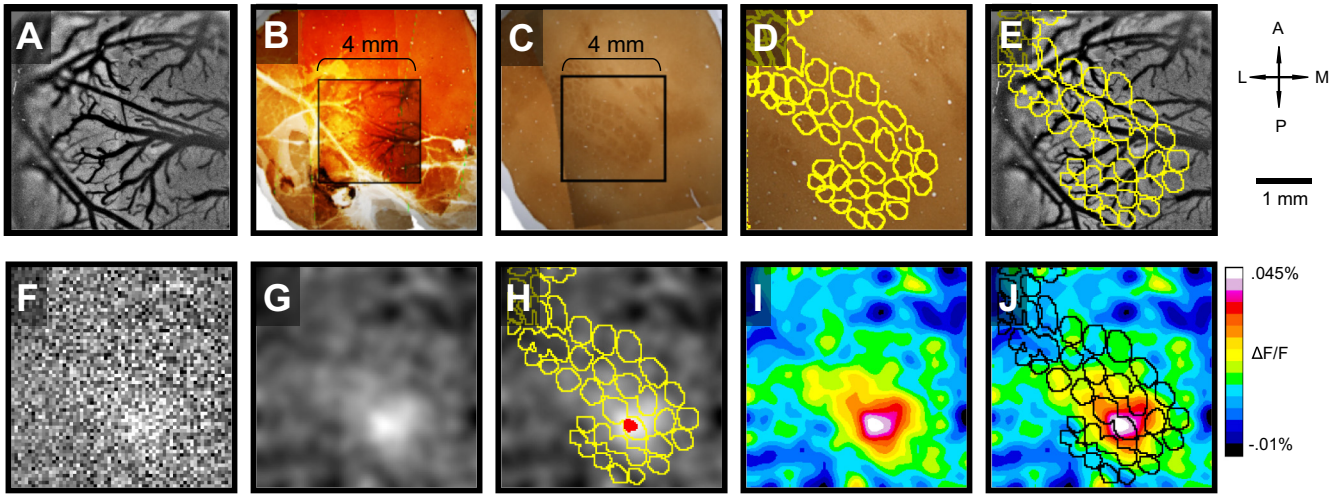

Fig. 1. Image alignment and processing. *A*: blood vessel map used for image alignment. Field of view (FOV) = 4 × 4 mm. *B*: camera FOV aligned with surface blood vessels on histological tissue. *C*: FOV extended to the subsequent sections of cortex stained for cytochrome oxidase, revealing the barrel field in layer 4. *D*: tracing of the barrel field. *E*: tracing of barrels superimposed on the FOV of the collected images. *F*: voltage-sensitive dye (VSD) subtraction image (see Fig 2 and MATERIALS AND METHODS) acquired 11.2 ms after whisker stimulation. *G*: image in *F* after Gaussian filtering with a sigma value of 2 pixels. *H*: image in *G* with aligned barrel field superimposed in yellow. Thresholded area of activation at 75% of peak amplitude response is colored red. *I*: image in *G* with level of activity (fluorescence, ΔF/F) illustrated by color intensity (see color scale, *right*). *J*: image in *I* with barrel field superimposed in black. For *A* and *D*–*J*, scale bar (*top right*) = 1 mm. A, anterior; P, posterior; M, medial; L, lateral.

cortex superimposed over the functional recordings, ROIs were selected with respect to individual barrels. To confirm functional image alignment with the histologically determined barrel field location, ROIs were also outlined using the initial area of activity after whisker stimulation (thresholded above 75–90% of peak activity). The area of initial activity, before spread of activity across the barrel field, lined up well with the primary barrel of an activated whisker (Fig. 1*H*). To ease visualization of functional activity, images were often scaled to a color map where warm to hot colors (orange, red, white) indicated the level of increased activity and cool to cold colors (green, blue, black) indicated the level of decreased activity (Fig. 1, *I* and *J*). Image analysis was performed using custom Matlab code (The MathWorks, Natick, MA) as well as ImageJ (http://rsbweb.nih.gov/ij/index.html) and FeatureJ (http://www.imagescience.org/meijering/software/featurej/).

Analysis of time course. ROIs were centered over individual barrels to assess a response of a barrel to whisker stimulation. To examine percent change in signal over time, functional images were derived by calculating the percent change in signal for each frame on a pixel-by-pixel basis. The first few frames, up to 70 ms before stimulation, were used as a baseline for (Fb − Fa)/Fa × 100, where Fa is the pixel fluorescence before stimulation and Fb represents the pixel fluorescence collected at a subsequent time point. Trial averaging was used to improve signal-to-noise ratio. Figure 2 shows two plots of a %ΔF time course. Figure 2*A* illustrates the raw averaged %ΔF on the *y*-axis plotted against the frame number (each frame 2.7 ms) on the *x*-axis for 100 trials of single whisker stimulation (black trace). Also plotted in Fig. 2*A* are the values collected for 100 blank trials (no stimulus, gray trace). The gradual decrease in VSD amplitude was a consequence of the photobleaching of the VSD and was the same in the blank and stimulus conditions. Figure 2*B* shows the response profile after the %F of the blank (Fig. 2*A*, gray trace) was subtracted from that of the single whisker stimulus condition (Fig. 2*A*, black trace), which removed the decay in fluorescence amplitude and revealed the change in fluorescence (%ΔF) caused by whisker stimulation. The response amplitude for each stimulus condition was measured from the peak response that typically occurred in a window 10–15 ms after stimulus onset (Fig. 2*B*, green bar).

Thresholding areas of activation and measuring centroid location. Because size and location of activation can be influenced by thresholding criteria, we examined activation sequences with different threshold criteria. As shown in Fig. 3, lower thresholds provide larger apparent activation zones (e.g., 50% threshold) and higher thresholds reveal smaller activations (e.g., 90% threshold). We based our threshold on two criteria: *1*) the latency to initial activation was consistent with electrophysiological studies, and *2*) the activation size was confined to the whisker barrel size. On this basis, we determined that 75% was the most appropriate threshold level. This criterion was also used in previous studies and agrees with the profile of activation spread from single barrels (in which activity in layer 2/3 is initially confined to a single barrel before spreading to the surrounding barrel field) revealed in previous electrophysiological studies (Armstrong-James et al. 1992; Ferezou et al. 2006; Petersen and Sakmann 2001; Petersen et al. 2003). The centroid for each frame's area of activity was determined by calculating the average of the *X* and *Y* coordinates for all the pixels with activations above threshold. To evaluate changes in the center of activation, *X* and *Y* coordinates were determined for the centroid of activation of the first frame of activity above threshold and the last frame of activity above threshold or when the area of activation dropped below the typical area size of a barrel. The coordinates for the centroid of activation for the first frame of activity above threshold were designated as the starting coordinates (SC = X_s, Y_s), whereas coordinates for the centroid of area of activation above threshold for the last frame were designated as ending coordinates (EC = X_e, Y_e).

To examine whether the centroid measurements were affected by the thresholding procedures, we also determined the centroid of activation by fitting, in a program written in LabVIEW (NI), the unfiltered VSD images with a two-dimensional Gaussian function with additional variables for baseline offset and Gaussian orientation. We report only the centroid measurements as determined by the thresholding procedures, since we found comparable shifts in centroid activity after reanalyzing all the data (average absolute difference in vector lengths and angles were 0.12 mm and 11.4°, respectively) and highly correlated centroid coordinates (average R^2 = 0.86). Furthermore, to gain an estimate of the variability of the centroid location during an imaging run, we generated half-maps by summing together different halves of the collected trials (even vs. odd trials or first half vs. second half). Although we only report findings based on average maps determined from all the trials within a run, we found that the average standard deviation within a run in the centroid location as determined from the *X* and *Y* coordinates from four half-maps (1 odd, 1 even, 1 first half, 1 second half) was only 0.121 mm (n = 3 experimental days, 15 whisker conditions multiplied by all centroid locations above 75% threshold value).

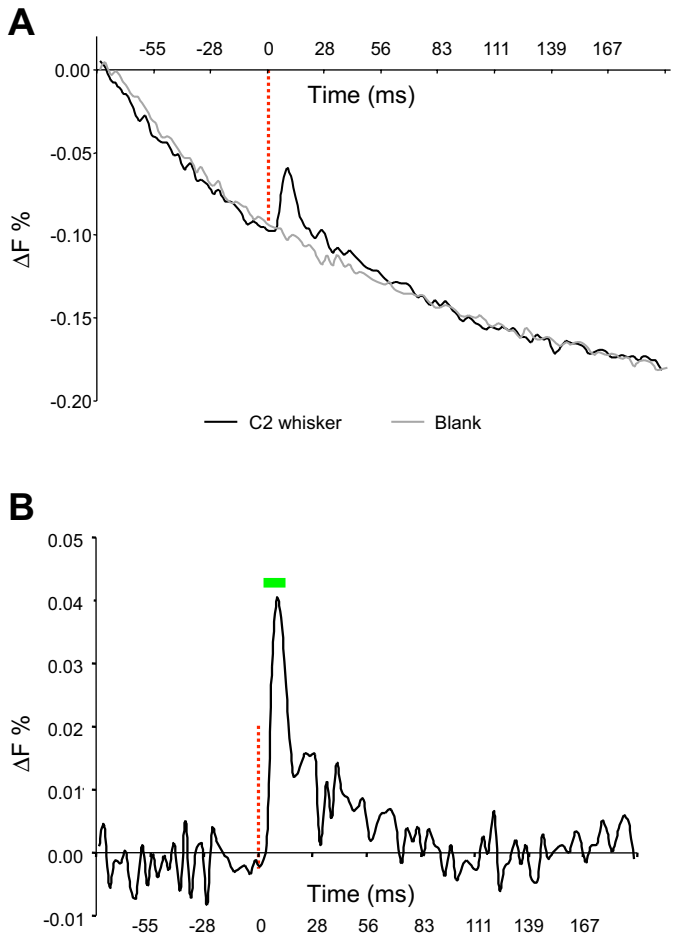

Fig. 2. Time course analysis. *A*: plot of VSD emission (ΔF) vs. time averaged for 100 trials of whisker stimulation (black line) and the blank condition (gray line) for a region of interest (ROI) centered over the C2 barrel. Decrease in VSD emission in both is a consequence of the photobleaching. Time of whisker stimulus for black plot is marked with a red dashed vertical line, and time course on the *x*-axis is aligned with the time of stimulus as 0 ms. *B*: plot showing the change in VSD signal due to whisker stimulation revealed by subtracting the blank condition (gray line in *A*) from the stimulus condition (black line in *A*) and thus removing the contribution of photobleaching from the signal. A time of 0 ms indicates the onset of whisker stimulation and is marked with a red dashed vertical line. The time period used in the measurement of peak response amplitude is indicated by the green bar.

RESULTS

VSD imaging provided the opportunity to evaluate at the population level spatial and temporal aspects of cortical barrel

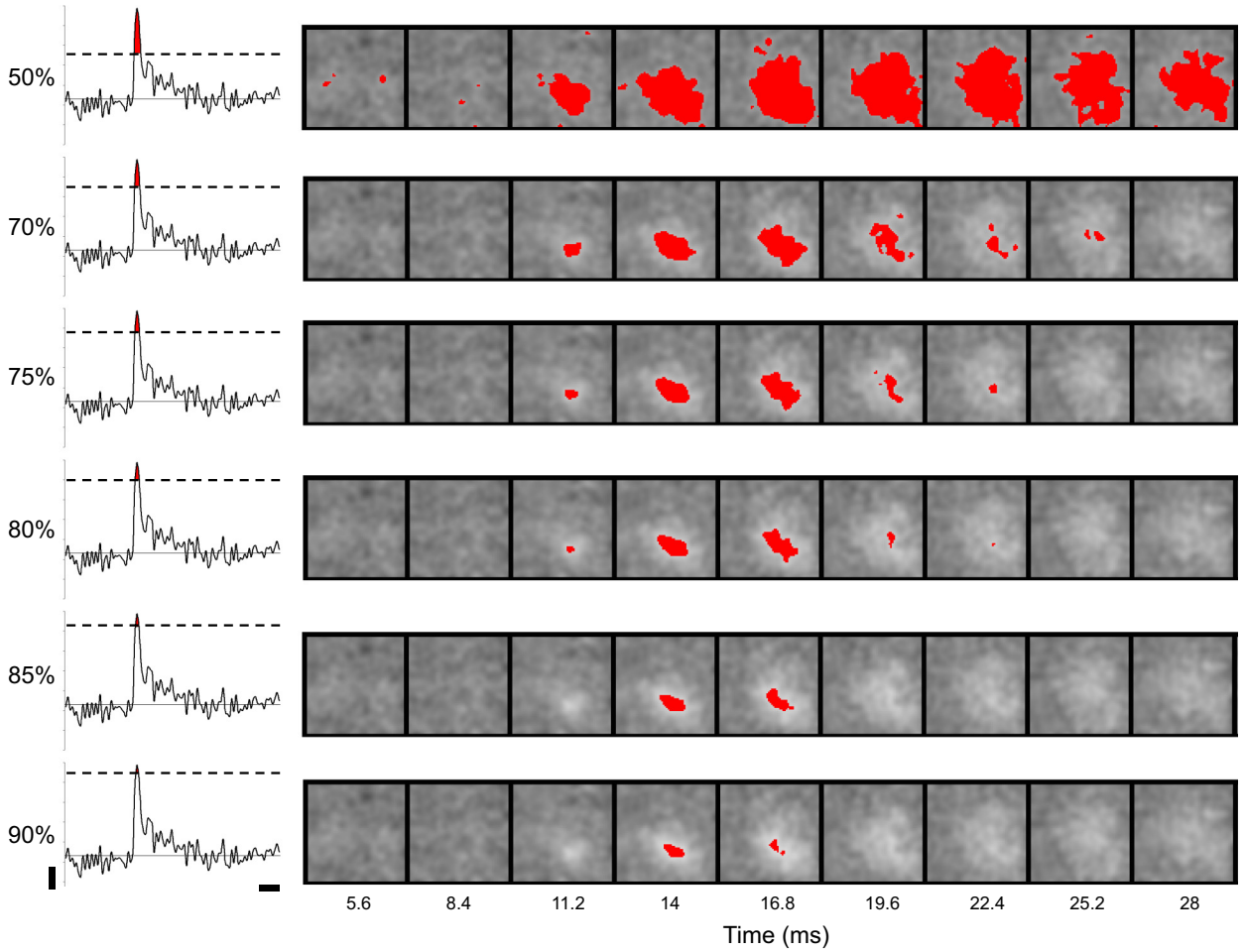

Fig. 3. Determining the appropriate threshold level. Areas of activation for C2 whisker response are shown for thresholds set at 50, 70, 75, 80, 85, and 90% of peak response. Notice how increasing the threshold level decreases the measured area of activation. We used 75% threshold to determine the first time point at which activation is evident (latency) because it is reproducibly significant, yet confined to a single barrel (see text). Scale bar for *y*-axis, $\Delta F = 0.01$; scale for *x*-axis, 30 ms.

response to whisker stimulation. In particular, we compared the time course and amplitude of responses to single and paired whisker stimulation and the accompanying spatial change of activation center over time.

Spatiotemporal response to single whisker stimulation. As a first step for evaluating our VSD images, we confirmed that the initial activity produced by single whisker stimulation was located over the topographically appropriate barrel in cortex. Previous studies of single whisker responses using VSD imaging reported that initial activity is confined to a single barrel in layer 2/3 before rapid spreading across cortex (Ferezou et al. 2006; Petersen and Sakmann 2001; Petersen et al. 2003; cf. Kleinfeld and Delaney 1996; Takashima et al. 2001; Tanifuji et al. 1994). Imaging frames captured 11.2 ms after whisker stimulation confirmed that initial activity was confined to a single whisker's corresponding barrel (Fig. 4, *A*–*C*). In Fig. 4*A*, barrels revealed with CO are outlined in white with the C2 barrel outlined in red. In response to C2 whisker stimulation, the sequence of activation shown in Fig. 4, *E* (pseudocolor activation maps) and *F* (maps thresholded at 75% overlaid on outlines of barrel field), was observed. The first frame (0 ms after whisker stimulation) shows the activity map at the onset of whisker stimulation. At that time the change in fluorescence in the ROI was near zero and comparable to spontaneous activity observed during the preceding 80 ms. Significant response to whisker stimulation began at the fifth frame (11.2 ms after whisker stimulation), resulting in a rise in fluorescence, localized over the C2 barrel. In the subsequent sixth and seventh frames (14 to 16.8 ms after whisker stimulation), activity quickly spread to surrounding barrels. Within a short time, from the fifth to the sixth frame (2.8 ms), the area of activation increased to more than twice the initial area. Thresholding images to 75% of peak revealed that peak activation, superimposed over the barrel field map (Fig. 4*F*), spread primarily along the stimulated whisker row and appeared to shift slightly toward the D whisker row of barrels before subsiding below threshold by 25 ms after whisker stimulation (Fig. 4*F*, ninth frame). Similar patterns were observed for C3 and C4 whisker stimulation (Fig. 4, *B* and *C*). For all three whiskers, initial activation within the barrels aligned well with the histology (Fig. 4*D*). The thresholded areas for the three whisker stimulations *1*) aligned well with their corresponding barrels, *2*) did not overlap with initial activation zones of other whisker stimulations, and *3*) aligned in an orderly manner within the barrel row. It is worth noting that when we looked at the thresholded area of initial activation (Fig. 4*D*) with respect to the barrels, the active area was actually smaller (at 75% threshold) than the size of a barrel [see Supplemental

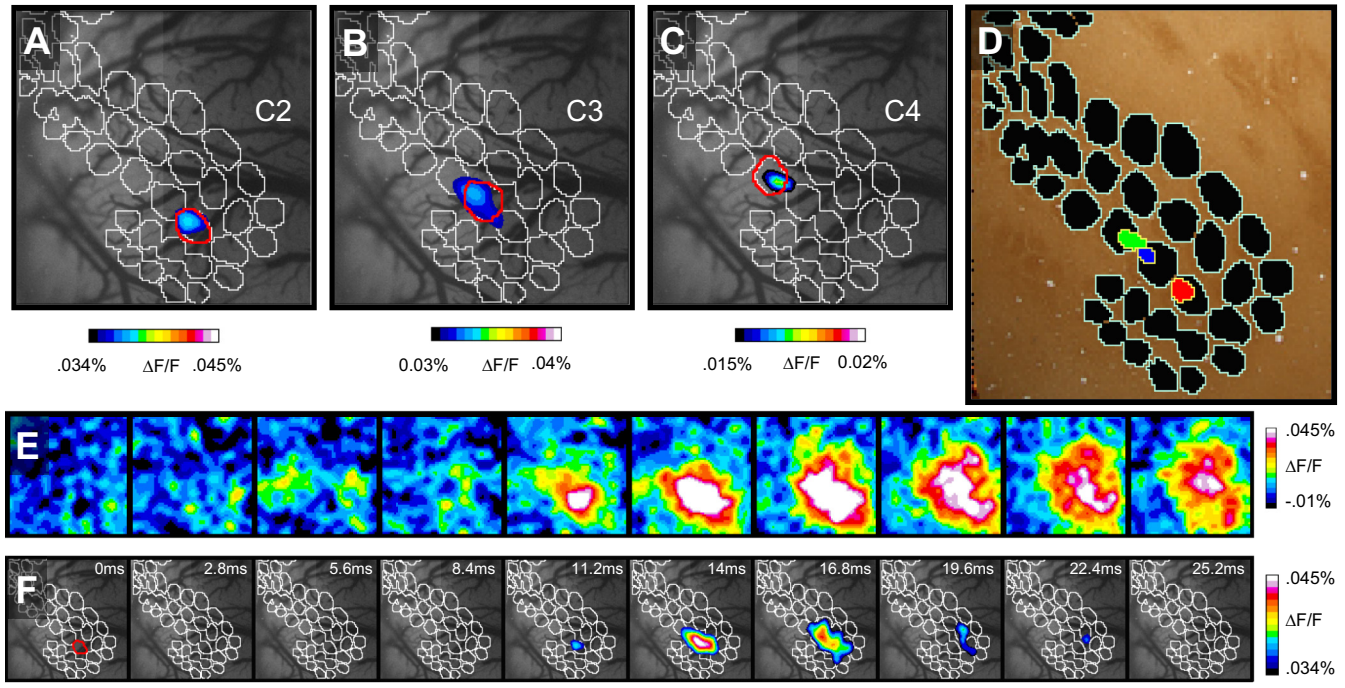

Fig. 4. Cortical response to a single whisker stimulation. *A–C*: the initial thresholded area and intensity of activation are shown for C2 (*A*), C3 (*B*) and C4 (*C*) whisker stimulation. Individual barrels (white outlines) are overlaid on the FOV blood vessel image. The stimulated whisker barrel is outlined in red. *D*: outlines of the initial areas of activation for C2 (red), C3 (blue), and C4 (green) whisker stimulation overlaid on the CO histology of the barrel field. Note that the initial areas of activation were confined to the barrel row representing the stimulated whiskers. *E*: sequence of color intensity images starting at the time of C2 whisker stimulation and ending 25.2 ms later (each frame = 2.7 ms), illustrating the spatiotemporal progression of cortical activation. *F*: intensity maps (*E*) after thresholding above 75% of peak activation superimposed over the barrel field (white outlines) and camera FOV. This sequence was produced from our second case, with signal averaged over 100 trials.

Movie 1 (supplemental data for this article is available online at the *Journal of Neurophysiology* website)].

In a single case with particularly good signal-to-noise ratio, we subdivided the trials to measure the degree of variability of the sub-barrel activation areas within the first frame of activity. For two runs where the C2 and C3 whiskers were stimulated, we divided our 100-trial data set into blocks of 10 (10 trials per block) and examined the degree of variability in intrabarrel location for this first frame. We found that the standard deviation of the intrabarrel location for C2 was 4.6 pixels on the *x*-axis(~288 μm) and 3.1 pixels on the *y*-axis (~194 μm), and for C3 the deviations were 2.1 pixels on the *x*-axis(~131 μm) and 3.5 on the *y*-axis (~219 μm) (i.e., both less than 300 $\times$ 250 μm, whereas the typical barrel size is approximately 500 $\times$ 440 μm or 8 $\times$ 7 pixels), indicating that the location of activation was stable within the respective barrels. For both the C2 and C3 barrels the activity was offset from the geometric center and located in the more rostral division of the barrel (see Fig. 4*D*, red and blue areas of activity). The presence of this offset indicates possible intrabarrel bias.

Spread of activity. Anatomic studies report more connections between barrels in a row than within an arc; consistent with this, VSD studies in mice and rats report spread of activity preferentially within a barrel row (Armstrong-James et al. 1992; Chapin 1986; Kleinfeld and Delaney 1996; Petersen et al. 2003). To examine whether there was preferential spread of activity to adjacent whisker barrels in our recordings, we used several ROIs to measure and compare the peak response amplitude in the four adjacent barrels (caudal, rostral, medial, lateral). Figure 5*A* shows peak response amplitude of activity averaged across all cases and across C2, C3, and C4 whisker stimulations for five ROIs: primary whisker (PW; yellow), rostral adjacent whisker (AW; red), caudal AW (blue), medial AW (green), and lateral AW (purple). As expected, the peak response amplitude in the PW barrel was significantly larger than other peak fluorescent measurements in adjacent barrels ($P < 0.0001$, Student's *t*-test). To confirm earlier reports of preferential spread of activity within a barrel row vs. a barrel arc, which is also in agreement with anatomic studies showing more connections within a row, we pooled the peak responses for the rostral and caudal adjacent barrels and the medial and lateral barrels to compare the peak response amplitudes within the barrel row and arc, respectively. Figure 5*B* shows the comparison of peak response amplitudes for the pooled adjacent arc and row barrels. The amplitude of fluorescence change was significantly greater in the stimulated barrel's adjacent row barrels than adjacent arc barrels, consistent with preferential spread within the barrel row (row vs. arc, $P < 0.05$, Student's *t*-test).

To rule out the possibility that the decline in activity in adjacent barrels was a consequence of uneven staining, we measured peak activation in the C2, C3, and C4 barrels in response to C2, C3, and C4 whisker stimulation. The response of a barrel to the primary whisker was always earlier and larger than responses to secondary whiskers. Thus the response amplitudes of surrounding barrels were not at an upper limit, supporting the conclusion that the spatiotemporal pattern of activity in response to stimulating a single whisker was not due to uneven dye staining.

Effects of dual whisker stimulation. Previous electrophysiological studies have reported that, compared with single whisker stimulation, dual whisker stimulation can have either a facilitatory or a suppressive effect depending on the interstimu-

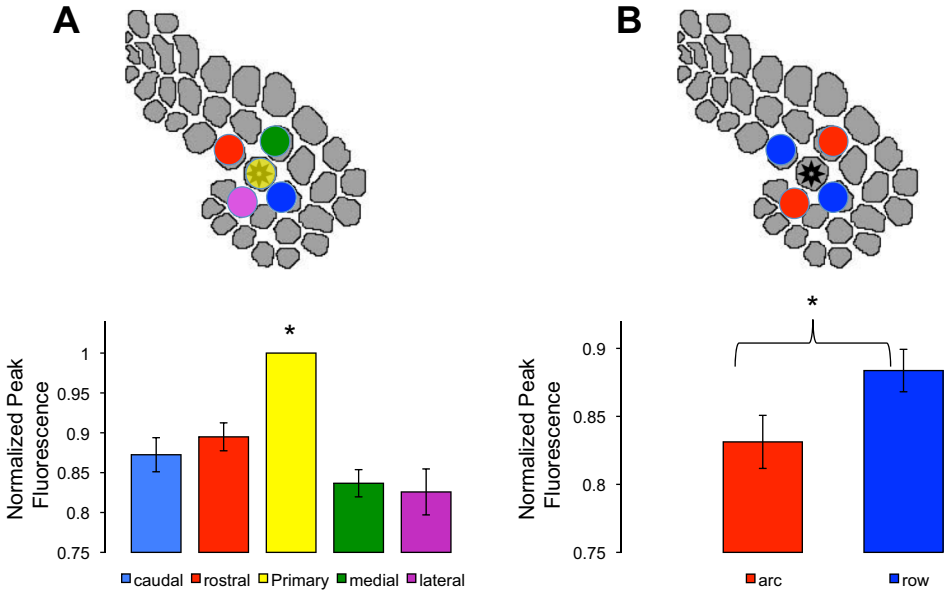

Fig. 5. Spread of activation greater along rows than arcs. *A*: map (*top*) shows the 5 ROIs used to measure. for a single whisker response, the peak amplitude of the primary (star, yellow) as well as the rostral (red), caudal (blue), medial (green), and lateral (purple) adjacent barrels. Bar graph (*bottom*) shows the peak amplitude responses for single whisker stimulations, normalized to the largest response and combined across all cases (ROI, mean, SE: caudal, 0.87, ±0.02; rostral, 0.89, ±0.02; medial, 0.84, ±0.02; lateral, 0.83, ±0.03; $n = 11$). The response for the primary barrel corresponding to the homologous stimulated whisker was significantly larger than the responses in all surrounding adjacent barrels (*$P < 0.0001$, Students *t*-test). *B*: map (*top*) shows the groupings of ROIs made to compare the peak amplitude of responses for adjacent barrels within the corresponding whisker arc (red) vs. the corresponding whisker row (blue). Bar graph (bottom) shows the normalized peak amplitude responses for the arc vs. row for all cases and all conditions (arc, 0.83, ±0.02; row, 0.88, ±0.02; $n = 11$). The response was significantly larger within the whisker row compared with the whisker arc (*$P < 0.05$, Students *t*-test).

lus interval (Mirabella et al. 2001; Shimegi et al. 1999). To examine the population response to multiwhisker stimulation, we compared the change in fluorescence responses for single and simultaneous dual whisker stimulation. Image sequences (acquired at 360 Hz) from one such experiment that included C2, C3, and paired C2/C3 stimulation are shown in Fig. 6. In each sequence, the time of whisker stimulation is highlighted by the frame outlined in bold. Using the peak amplitude

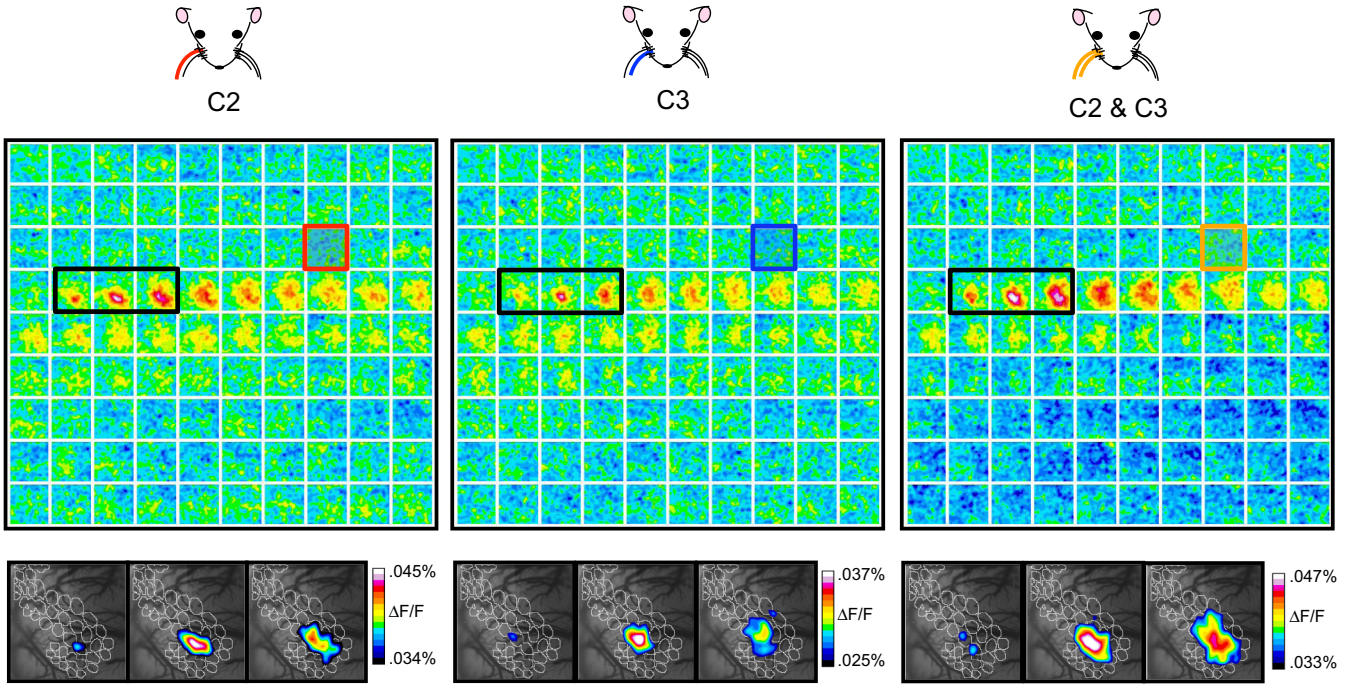

Fig. 6. *Top*: Montages of time courses of activation for C2 (*left*), C3 (*middle*), and paired C2+C3 whisker activation (*right*). Colored bold outline indicates time of whisker stimulation. Images were acquired at 360 Hz. Before whisker stimulation, cortical reflectance was at baseline levels (primarily blue and green). After whisker stimulation, barrel-specific activation (yellow and red) was first seen at around 11 ms, followed by spread of activity to surrounding regions (20–30 ms), after which there was a return to baseline levels. *Bottom*: first 3 frames of thresholded activation (black bold outline in montages above) superimposed over the vessel map from the imaging FOV with the barrel field outlines in white as in Fig. 4*F*.

response (see Fig. 2*B*), we found the response for paired whisker stimulation under these conditions was significantly sublinear ($P < 0.001$, Students *t*-test). Pooling measurements for all cases ($n = 4$) gave population responses for the PW, AW, paired PW+AW, and linear sum conditions. As quantified in Fig. 7, across cases we found *1*) PW responses were significantly greater than AW responses ($P < 0.01$, Students *t*-test), *2*) paired PW+AW responses were significantly greater than PW responses ($P < 0.01$, Students *t*-test), and *3*) paired PW+AW responses were significantly smaller than the linear sum of single AW and PW responses ($P < 0.001$, Students *t*-test), indicating sublinear summation. Collectively these findings point toward a spatiotemporal inhibitory process leading to sublinear responses to paired stimulation, in agreement with the reported effect of paired stimulation in mouse VSD recordings (Civillico and Contreras 2006).

Shifting centroid of activation. As shown in Fig. 4, the area of evoked activity showed a distinct pattern of activation, starting with a small focal area of activity (11.2 ms poststimulus) centered over the principal whisker's barrel, rapidly expanding primarily within a barrel row (12–18 ms), followed by a decline in area of activation (20–25 ms) and return to baseline. Surprisingly, the center of activation appeared to shift over time. In Fig. 8*A*, the center of activity (75% threshold) shifted from the C2 barrel (first frame) toward a location roughly between the C2 and C3 (second frame), then toward a location more in the septal area between the C2 and D2 barrels (third frame), and then into the D2 barrel itself (fourth and fifth frames) (see Fig. 8*B* and Supplemental Movie 2). As shown in Fig. 8*C*, overlaying the earliest frame of activity above threshold (11.2 ms after stimulus onset) and the final frame of activity above threshold (22.4 ms after stimulus onset) revealed a clear spatial shift in the location of activation. The shift in activation was confirmed by plotting time courses of activation at the initial (SC, blue) and final (EC, red) centers of activation above threshold (Fig. 8*D*). Plotting the change in fluorescence (above threshold activity over time) for the two ROIs revealed two temporally distinct peaks of activation indicative of a clear shift in activation over both space and time. This shift was not simply due to variability of signal. In fact, at 75% threshold, in the first frame, activity was centered on the initial start point (SC ROI) and had not yet reached the end point (EC ROI); in the last two frames, activity had fallen below threshold at the start point but was still above threshold in the end point (Fig. 8*D*). This is consistent with a true shift in center of activation.

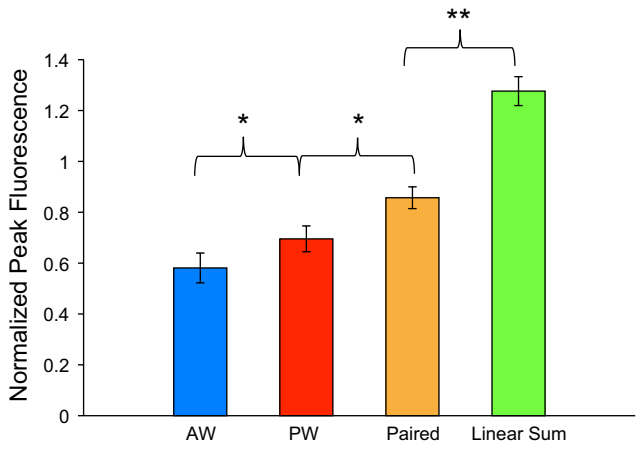

Fig. 7. Sublinear effect of simultaneous paired whisker stimulation. Bar graph shows peak amplitude of responses in a single ROI over the principal whisker barrel to principal whisker (PW), adjacent whisker (AW), and paired whisker (AW+PW) and the linear sum of single AW and PW responses. Responses were normalized to the peak response across conditions and then pooled across all cases. The response to paired whisker stimuli was significantly greater than single PW or AW conditions (*$P < 0.01$, paired vs. PW and paired vs. AW; Students *t*-tests). The linear sum of AW and PW responses was significantly larger than the observed paired responses (**$P < 0.0001$, paired vs. linear sum; Students *t*-test). Data are condition, mean, SE: AW, 0.58, ±0.06; PW, 0.70, ±0.05; paired, 0.86, ±0.04; linear sum, 1.28, ±0.06; $n = 11$ whisker pairings.

We examined whether this shift occurred across all cases and whether it occurred under both single and dual whisker stimulation conditions. If the spread of activity was determined by the intrinsic connectivity of the barrel cortex (i.e., preferential spread within the row), then the expectation would be that the shift in activity over time would be similar for single or paired whisker stimulations. We found that shifts in activation center occurred consistently across cases and, furthermore, that this shift tended to occur in the posteromedial direction toward the more ventral whisker row and more caudal whisker arc. The mean distance of the shift was 1.2 mm ($n = 15$) with 100% (15/15) of the shifts moving toward the more ventral whisker row and 80% (12/15) of the shifts moving toward the more caudal whisker arcs. There was no significant difference in the mean distance of the shift between paired and single stimulations. Figure 9*A* illustrates the shift from start point (large colored dot) to the end point (small colored dot) for three single whisker stimulation cases. After C2 whisker stimulation (*top left*, 3 cases), activation centers shifted toward the D whisker row. After C3 whisker stimulation (*top middle*, 3 cases), activation centers also shifted to the D whisker row. After C4 whisker stimulation (*top right*), activation shifted clearly toward the D whisker row in one case and toward the C3 whisker barrel in two cases. Moreover, such shifts were also observed under dual whisker stimulation conditions. Six cases are shown in Fig. 9*A* (*bottom left*, 3 cases C2+C3; *bottom right*, 3 cases C3+C4). A summary of all cases (both single and dual whisker stimulation conditions) is shown in Fig. 9*B*. All cases are displayed so that the primary whisker barrel is centered over the C3 barrel. We observed that all activations shifted toward the more ventral whisker rows (D and E rows, blue and purple), with no shift toward the more dorsal whisker rows (A and B rows, orange and red). Shifts toward caudal arcs were also more common than shifts toward anterior arcs. Thus our 15 cases showed an overall trend for shift in activation in the posteromedial direction of cortex toward the more ventral whisker rows and more caudal whisker arcs. Such a directional shift is consistent with known anisotropies in underlying interbarrel connections (see DISCUSSION).

DISCUSSION

We used VSD imaging to examine cortical activity population responses to single and simultaneous dual whisker deflections in urethane-anesthetized rat barrel cortex. We found that activation to single whisker stimulation originated at the principal whisker barrel and quickly (within 20 ms) spread extensively to surrounding regions. This spread was oriented preferentially along a barrel row. Paired whisker stimulation produced a significant sublinear summation compared with stimulation of two adjacent whiskers individually. Surprisingly, in response to both single and dual whisker stimulation,

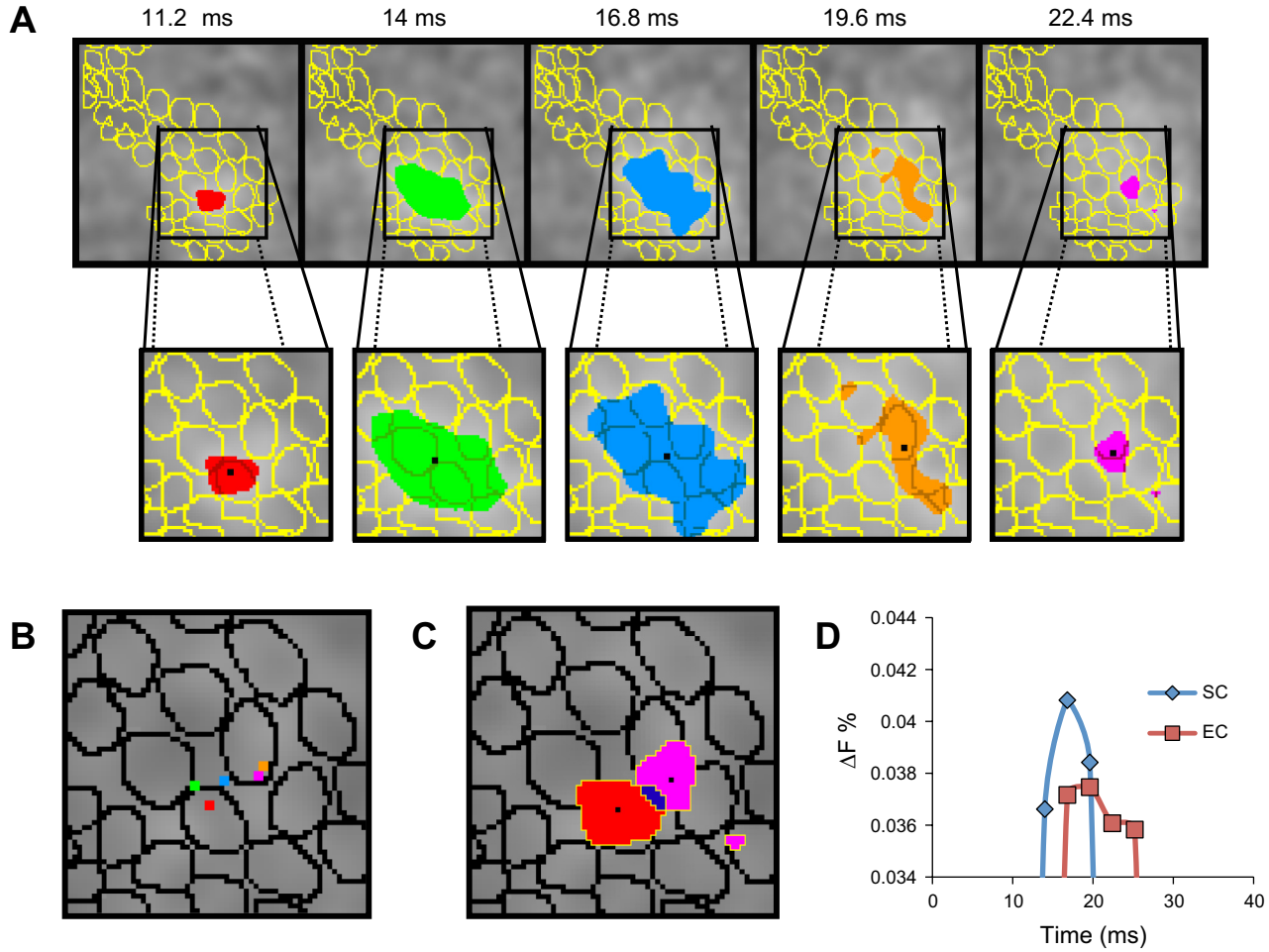

Fig. 8. Shift in centroid location over time. *A*: VSD image sequence shows the area of activation thresholded above 75% of peak response for C2 whisker stimulation overlaid on an outline of the barrel fields. Activation was above threshold for 5 frames, starting 11.2 ms after whisker stimulation and ending 22.4 ms after stimulation onset. The area of activation above threshold for each frame is magnified in *insets* with the centroid of the area of activation for each frame marked with a black dot. Area of activation is colored differently for each frame. *B*: trajectory of the centroid shift in location over time. Each centroid spot is colored the same as its activation area represented in the frames in *A*. *C*: magnified areas of activation for the first and last frames of activity above threshold are overlaid on the barrel field with their respective centroids of activation marked in black. Notice the clear spatial shift in location of the area of activation. *D*: a plot of the change in fluorescence (ΔF) over time for 2 ROIs shows temporally distinct peaks of activation indicative of a spatial shift in activity. The first ROI is over the centroid of activation for the first frame (starting coordinates, SC; blue), and the second ROI is located over the centroid of activation for the last frame of activation (end coordinates, EC; red). Plots of ΔF over time are only for activation thresholded above 75% of peak response (0.034%).

we consistently found a spatial shift of the centroid of activity in the barrel field, one that occurred over 10–20 ms and offset as far as 1–2 barrels as the activity faded. This shift occurred predominantly in the posteromedial direction of barrel cortex.

Spatiotemporal responses. The VSD imaging responses to whisker stimulation measured in barrel cortex showed several spatiotemporal characteristics consistent with previous studies. In the temporal structure of the images, detecting responses as early as 11 ms after whisker stimulation corresponded with the known timing of excitatory activity reaching layer 2/3 of cortex (Armstrong-James et al. 1992). The spatial profile of the VSD images showed initial focal activity roughly the diameter of a barrel column (~400 μm) followed by a rapid horizontal spread preferentially within a whisker row and then to surrounding cortex, in agreement with previous studies (Kleinfeld and Delaney 1996; Petersen and Sakmann 2001). Similarly, in previous studies using electrophysiology and VSD imaging of barrel cortex, it was shown that responses start in layer 4 of barrels, progress vertically directly above the barrel into layer 2/3, and then spread horizontally in layer 2/3 in a "pagoda like" manner (Kleinfeld and Delaney 1996; Lippert et al. 2007; Petersen and Sakmann 2001; Tanifuji et al. 1994).

We did note in a single case with particularly good signal-to-noise ratio that the initial area of activation above threshold was confined to an area within the single barrel. Because the signal-to-noise ratio for the two barrels was exceptionally strong, we were able to subdivide the trials to measure the degree of variability of sub-barrel activation area. For both, the center of activation was located rostral from the geometric center of the barrel, consistent with our caudal-to-rostral direction of whisker stimulation. Thus, based on the data analysis from these two barrels, our results could be consistent with the presence of an intrabarrel somatotopic directional map (Andermann and Moore 2006; Kerr et al. 2007; Kremer et al. 2011). However, the results from two barrels with exceptional signal-to-noise ratio are far from conclusive and further studies are needed (Tsytsarev et al. 2010a, 2010b).

The barrel responses presently reported with VSD imaging were monophasic. Other reports using VSD imaging report a

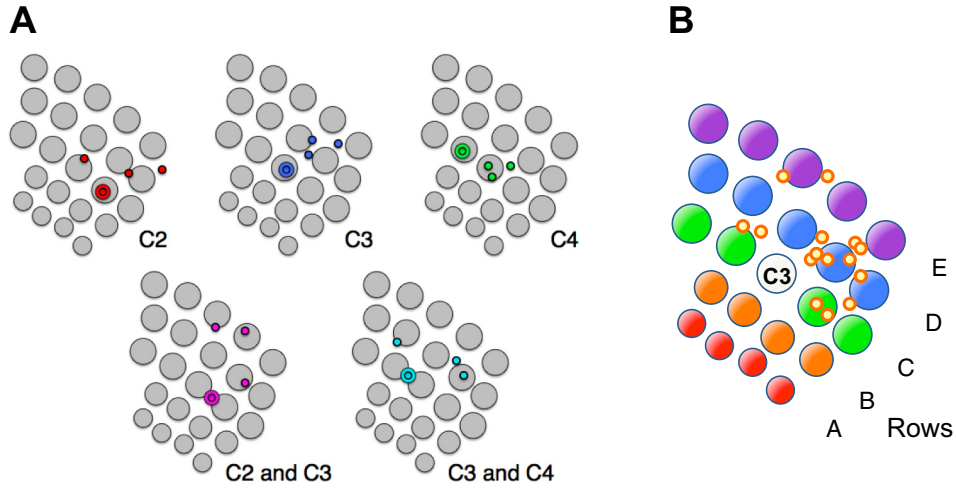

Fig. 9. Coordinates for shift in centroids of activation above threshold for each condition. *A*: for each condition (C2, red; C3, blue; C4, green; C2 and C3, purple; C3 and C4, turquoise) across 3 cases, the locations of the initial coordinates for the centroid of activity above threshold are plotted on a model barrel field (larger circles), whereas the final coordinates for the centroids of areas of activation above threshold are plotted as smaller circles. *B*: the trend for shift of activation with respect to whisker rows (*left*) is shown by collapsing the starting coordinates for all conditions onto the center of the C3 barrel and plotting their respective end coordinates due to shift of the centroid of activation over time. Notice the shift in activity appears to move primarily in the posteromedial direction (toward the more ventral whisker rows and caudal whisker arcs).

triphasic response (Derdikman et al. 2003). This difference was likely due to our stimulus parameters. Derdikman et al. (2003) found the profile of barrel response varied with different stimulus intensities and durations. They found a monophasic response for weak stimuli, whereas stronger stimulation led to a triphasic response. In particular, presentation of a 1-ms deflection evoked a late hyperpolarization, whereas whisker deflections of longer durations, 10 and 30 ms, did not (Derdikman et al. 2003). Thus our finding that the ~250-to 300-μm whisker deflections for the duration of 20 ms we used induced monophasic responses is consistent with previous studies.

Paired stimulation. The study of cortical responses to paired simultaneously stimulated whiskers was designed to examine how multiple foci of activity were integrated in cortex. Previous studies have found both facilitatory and suppressive effects. In the study by Shimegi et al. (1999), the facilitatory or suppressive effect was dependent on the timing between whisker stimulation. For example, a population of layer 2/3 cells recorded in rats showed facilitation of firing rate with paired whisker stimulations, either simultaneously or with a <20-ms (maximum facilitation at 4 ms) interval between successive whisker stimuli. In the same study, Shimegi and colleagues reported suppressive effects when the timing between adjacent whisker stimuli was >20 ms. Mirabella et al. 2001 found some slight facilitation to paired whisker stimuli but primarily a sublinear summation when they stimulated an increasing number of whiskers, indicative of suppressive effects.

To date, the bulk of studies on simultaneous stimulation of multiple whiskers report suppressive effects (Brumberg et al. 1996; Civillico and Contreras 2006; Ego-Stengel et al. 2005; Higley and Contreras 2003, 2005; Webber and Stanley 2004). What has become clear is that the nature of cortical interactions is crucially dependent on the timing between whisker deflections on a millisecond timescale (Shimegi et al. 1999; Simons and Carvell 1989; see also subcortical effects, Roy et al. 2011; Simons 1983, 1985; Simons and Carvell 1989). In our study, simultaneous stimulation of whiskers produced sublinear summation of the VSD signal in barrel cortex. These results are consistent with the bulk of previous studies and parallel a similar VSD study conducted in the mouse barrel field (Civillico and Contreras 2006). Thus the findings point to a common feature of cortical processing in whisker somatosensory systems of the two rodent species, despite the anatomic differences identified above.

Spatiotemporal shift of activation in barrel cortex. To our knowledge, this is the first report in rodent barrel cortex of substantial shifts in location of the center of activation in response to single whisker stimulation. Although there are reports of shifting activations within single barrels (Andermann and Moore 2006) and asymmetries of inputs to single barrels (Furuta et al. 2011), these and other studies specifically note that the center of activation remains essentially the same and the spread is isotropic across the row. Some intracellular studies have shown a later onset of subthreshold activation from surround vibrissal inputs, from which one could infer a shift (Moore and Nelson 1998). Otherwise, there is one study, using multi-array recordings in layer 5, that illustrated shifts (Fig. 6 in Ghazanfar and Nicolelis 1999). Outside of this one report, this is the first observation of the center of activation (albeit at a population level) shifting from one barrel to or toward another and, moreover, that this shift occurs across barrels with a tendency in the caudal-ventral direction.

Although this finding was unexpected, we propose that such shifts may be consistent with known functional and anatomic asymmetries in rat barrel cortex. In 1989 Simons and Carvell reported functional asymmetries in single-unit recordings in the barrel field. They found that the caudally adjacent whisker evoked more inhibition on principal whisker barrel neurons than the rostrally adjacent whisker; furthermore, the ventral adjacent whisker evoked more inhibition than the dorsal whisker (Simons and Carvell 1989). This asymmetry was later confirmed in the responses of inhibitory interneurons (fast spiking units) and the observed gradient of inhibitory effect produced on regular spiking units (Simons 1995). These effects were not evident in subcortical ventroposterior medial thalamic projection neurons, suggesting the asymmetric gradient of inhibition was established in cortex (Brumberg et al. 1996).

Consistent with these functional findings, there are anatomic asymmetries in the projections of cortical axons in the barrel fields. Bernardo et al. (1990a and 1990b) reported intracortical connections are stronger between barrels in the same row than between rows and, moreover, a large directional bias in connections toward the more anterior barrel row in cortex (corresponding to the more ventral whisker row on the face, closer to the mouth). The asymmetries in connections coupled with the

functional asymmetries in inhibition are further confirmed in early 2-deoxyglucose (2-DG) studies in behaving animals where the majority of activation was observed in the barrels of the more ventral and caudal whiskers, followed by a clear global gradient of declining activity toward the barrels of the more dorsal and rostral whiskers (McCasland et al. 1991).

Our data add an interesting temporal component to these spatial relationships. First, we suggest that the anisotropic connections within barrel rows are likely to underlie our observed preferential spread of VSD signal along, rather than across, rows. We also propose that the temporal posteromedial shift derives from the presence of stronger anatomic connections with anterior than posterior barrel rows. The tendency for activity to move in the posteromedial direction (toward the ventral and caudal whiskers) would further explain the enhanced activity in these barrels found with 2-DG studies. Furthermore, the time course of this shift is consistent with delays associated with the interbarrel propagation of activity. Under normal whisking conditions, the summation of spreading excitatory postsynaptic potentials (EPSPs) toward the posteromedial direction in cortex (i.e., the ventral and caudal whiskers) would bring the potentials closer to threshold, leading to higher firing rates, which results in higher activity of these barrels with respect to the entire barrel field. Such a functional bias could be important for integrating salient sensory information from the ventral/caudal large vibrissae close to the mouth.

Analysis of the location of the centroid of activation above threshold over time found a preferential shift of the center of activation toward the more ventral whisker rows and more caudal whisker arcs. These findings suggest that the inhibitory component of a barrel response is stronger in the lateral portion of the barrel field, resulting in activity above threshold being sustained longer and spread preferentially into the ventral/caudal whisker barrels (Chagnac-Armitai and Conners 1989). This effect could be related to the optimal sequence of whisker stimulation (Ghazanfar and Nicolelis 1999; Kleinfeld and Delaney 1996), as well as being based on the intracolumnar connections.

Updated view of spatiotemporal events in barrel cortex following whisker stimulation. Our VSD imaging supports a model with the following sequence of events after whisker stimulation: *1*) an initial short-latency, high-amplitude excitatory response in cortical layers 2/3 as well as layer IV, based largely on thalamocortical projections to layer 4, and limited to the confines of the corresponding barrel of the stimulated vibrissae; *2*) activity quickly spreading to the surrounding barrels, allowing for an integration of responses of nearly simultaneous whisker stimulations (<20 ms) resulting in an enhancement of excitatory amplitudes, especially in layer 2/3; and *3*) a rapid directional shift of activation in the population determined by timing of whisker contact, influenced by inherent biases in anatomic connection patterns and spatial distribution of inhibitory influences. This directional bias may have behavioral relevance, since it could lead to preferential amplification of sensory stimulation of larger whiskers near the mouth.

ACKNOWLEDGMENTS

We thank Lisa Chu and Alyssa Zuehl for excellent technical assistance and Kristof Giber for participation in some experiments.

GRANTS

This research was supported by National Institute of Neurological Disorders and Stroke Grants NS044375 (to A. W. Roe) and NS052821 (to A. W. Roe) and the Center for Integrative and Cognitive Neuroscience.

DISCLOSURES

No conflicts of interest, financial or otherwise, are declared by the authors.

AUTHOR CONTRIBUTIONS

B.R.L., R.M.F., and J.E.W. performed experiments; B.R.L. analyzed data; B.R.L., R.M.F., and A.W.R. interpreted results of experiments; B.R.L. and R.M.F. prepared figures; B.R.L. and R.M.F. drafted manuscript; B.R.L., R.M.F., F.F.E., and A.W.R. edited and revised manuscript; B.R.L., R.M.F., J.E.W., F.F.E., and A.W.R. approved final version of manuscript; R.M.F., F.F.E., and A.W.R. conception and design of research.

REFERENCES

Alloway KD. Information processing streams in rodent barrel cortex: the differential functions of barrel and septal circuits. *Cereb Cortex* 18: 978–989, 2008.

Andermann ML, Moore CI. A somatotopic map of vibrissa motion direction within a barrel column. *Nat Neurosci* 9: 543–551, 2006.

Armstrong-James M, Fox K. Spatiotemporal convergence and divergence in the rat S1 "barrel" cortex. *J Comp Neurol* 263: 265–281, 1987.

Armstrong-James M, Fox K, Das GA. Flow of excitation within rat barrel cortex on striking a single vibrissa. *J Neurophysiol* 68: 1345–1358, 1992.

Bernardo KL, McCasland JS, Woolsey TA, Strominger RN. Local intra- and interlaminar connections in mouse barrel cortex. *J Comp Neurol* 291: 231–255, 1990a.

Bernardo KL, McCasland JS, Woolsey TA. Local axonal trajectories in mouse barrel cortex. *Exp Brain Res* 82: 247–253, 1990b.

Brecht M, Sakmann B. Dynamic representation of whisker deflection by synaptic potentials in spiny stellate and pyramidal cells in the barrels and septa of layer 4 rat somatosensory cortex. *J Physiol* 543: 49–70, 2002.

Brumberg JC, Pinto DJ, Simons DJ. Spatial gradients and inhibitory summation in the rat whisker barrel system. *J Neurophysiol* 76: 130–140, 1996.

Bruno RM, Simons DJ. Feedforward mechanisms of excitatory and inhibitory cortical receptive fields. *J Neurosci* 22: 10966–10975, 2002.

Bureau I, von Saint Paul F, Svoboda K. Interdigitated paralemniscal and lemniscal pathways in the mouse barrel cortex. *PLoS Biol* 4: e382, 2006.

Cayce J, Friedman RM, Jansen D, Mahavaden-Jansen A, Roe AW. Pulsed infrared light alters neural activity in rat somatosensory cortex in vivo. *Neuroimage* 57: 155–166, 2011.

Chagnac-Amitai Y, Connors BW. Horizontal spread of synchronized activity in neocortex and its control by GABA-mediated inhibition. *J Neurophysiol* 61: 747–758, 1989.

Chapin JK. Laminar differences in sizes, shapes, and response profiles of cutaneous receptive fields in the rat SI cortex. *Exp Brain Res* 62: 549–559, 1986.

Civillico E, Contreras D. Integration of evoked responses in supragranular cortex studied with optical recordings in vivo. *J Neurophysiol* 96: 336–351, 2006.

Derdikman D, Hildesheim R, Ahissar E, Arieli A, Grinvald A. Imaging spatiotemporal dynamics of surround inhibition in the barrels' somatosensory cortex. *J Neurosci* 23: 3100–3105, 2003.

Ego-Stengel V, Mello e Souza T, Jacob V, Shulz DE. Spatiotemporal characteristics of neuronal sensory integration in the barrel cortex of the rat. *J Neurophysiol* 93: 1450–1467, 2005.

Ferezou S, Bolea C, Petersen CC. Visualizing the cortical representation of whisker touch: voltage-sensitive dye imaging in freely moving mice. *Neuron* 50: 617–629, 2006.

Furuta T, Deschenes M, Kaneko T. Anisotropic distribution of thalamocortical boutons in barrels. *J Neurosci* 31: 6432–6439, 2011.

Ghazanfar AA, Nicolelis MA. Spatiotemporal properties of layer V neurons of the rat primary somatosensory cortex. *Cereb Cortex* 9: 348–361, 1999.

Higley MJ, Contreras D. Nonlinear integration of sensory responses in the rat barrel cortex: an intracellular study in vivo. *J Neurosci* 23: 10190–10200, 2003.

Higley MJ, Contreras D. Integration of synaptic responses to neighboring whiskers in rat barrel cortex in vivo. *J Neurophysiol* 93: 1920–1934, 2005.

Jin WJ, Zhang Wu JY RJ. Voltage-sensitive dye imaging of population neuronal activity in cortical tissue. *J Neurosci Methods* 115: 13–27, 2002.

Kerr J, de Kock C, Greenberg D, Bruno R, Sakmann B, Helmchem F. Spatial organization of neuronal population responses in layer 2/3 of rat barrel cortex. *J Neurosci* 27: 13316–13328, 2007.

Kim U, Ebner FF. Barrels and septa: separate circuits in rat barrels field cortex. *J Comp Neurol* 408: 489–505, 1999.

Kleinfeld D, Delaney KR. Distributed representation of vibrissa movement in the upper layers of somatosensory cortex revealed with voltage-sensitive dyes. *J Comp Neurol* 375: 89–108, 1996.

Kremer Y, Leger JF, Goodman D, Brette R, Bourdieu L. Late emergence of the vibrissa direction selectivity map in the rat barrel cortex. *J Neurosci* 31: 10689–10700, 2011.

Lippert MT, Takagaki K, Xu W, Huang X, Wu JY. Methods for voltage-sensitive dye imaging of rat cortical activity with high signal-to-noise ratio. *J Neurophysiol* 98: 502–512, 2007.

Manns ID, Sakmann B, Brecht M. Sub- and suprathreshold receptive field properties of pyramidal neurones in layers 5A and 5B of rat somatosensory barrel cortex. *J Physiol* 556: 601–622, 2004.

McCasland JS, Carvell GE, Simons DJ, Woolsey TA. Funtional asymmetries in the rodent barrel cortex. *Somatosens Mot Res* 8: 111–116, 1991.

Mirabella G, Battiston S, Diamond M. Integration of multiple-whisker inputs in rat somatosensory cortex. *Cereb Cortex* 11: 164–170, 2001.

Moore CI, Nelson SB. Spatio-temporal subthreshold receptive fields in the vibrissa representation of rat primary somatosensory cortex. *J Neurophysiol* 80: 2882–2892, 1998.

Petersen C, Sakmann B. Functionally independent columns of rat somatosensory barrel cortex revealed with voltage-sensitive dye imaging. *J Neurosci* 21: 8435–8446, 2001.

Petersen CC, Grinvald A, Sakmann B. Spatiotemporal dynamics of sensory responses in layer 2/3 of rat barrel cortex measured in vivo by voltage-sensitive dye imaging combined with whole-cell voltage recordings and neuron reconstructions. *J Neurosci* 23: 1298–1309, 2003.

Roy NC, Bessaih T, Contreras D. Comprehensive mapping of whisker-evoked responses reveals broad, sharply tuned thalamocortical input to layer 4 of barrel cortex. *J Neurophysiol* 105: 2421–2437, 2011.

Shimegi S, Ichikawa T, Akasaki T, Sato H. Temporal characteristics of response integration evoked by multiple whisker stimulations in the barrel cortex of rats. *J Neurosci* 19: 10164–10175, 1999.

Shimegi S, Akasaki T, Ichikawa T, Sato H. Physiological and anatomical organization of multiwhisker response interactions in the barrel cortex of rats. *J Neurosci* 20: 6241–6248, 2000.

Simons DJ. Multi-whisker stimulation and its effects on vibrissa units in rat SmI barrel cortex. *Brain Res* 276: 178–182, 1983.

Simons DJ. Temporal and spatial integration in the rat SI vibrissa cortex. *J Neurophysiol* 54: 615–635, 1985.

Simons DJ, Carvell GE. Thalamocortical response transformation in the rat vibrissa/barrel system. *J Neurophysiol* 61: 311–330, 1989.

Simons DJ, Woolsey TA. Morphology of Golgi-Cox-impregnated barrel neurons in rat SmI cortex. *J Comp Neurol* 230: 119–132, 1984.

Takashima I, Kajiwara R, Iijima T. Voltage-sensitive dye versus intrinsic signal optical imaging: comparison of optically determined functional maps from rat barrel cortex. *Neuroreport* 12: 2889–2894, 2001.

Tanifuji M, Sugiyama T, Murase K. Horizontal propagation of excitation in rat visual cortical slices revealed by optical imaging. *Science* 266: 1057–1059, 1994.

Tsytsarev V, Pope D, Pumbo E, Garver W. Intrinsic optical imaging of directional selectivity in rat barrel cortex: application of a multidirectional magnetic whisker stimulator. *J Neurosci Methods* 189: 80–83, 2010a.

Tsytsarev V, Pope D, Pumbo E, Yablonskii A, Hofmann M. Study of the cortical representation of whisker directional deflection using voltage-sensitive dye optical imaging. *Neuroimage* 53: 233–238, 2010b.

Veinante P, Deschenes M. Single- and multi-whisker channels in the ascending projections from the principal trigeminal nucleus in the rat. *J Neurosci* 19: 5085–5095, 1999.

Webber RM, Stanley GB. Nonlinear encoding of tactile patterns in the barrel cortex. *J Neurophysiol* 91: 2010–2022, 2004.

Welker C, Woolsey TA. Structure of layer IV in the somatosensory neocortex of the rat: description and comparison with the mouse. *J Comp Neurol* 158: 437–453, 1974.

Wong-Riley M. Changes in the visual system of monocularly sutured or enucleated cats demonstrable with cytochrome oxidase histochemistry. *Brain Res* 171: 11–28, 1979.

Woolsey TA, Van der Loos H. The structural organization of layer IV in the somatosensory region (SI) of mouse cerebral cortex. The description of a cortical field composed of discrete cytoarchitectonic units. *Brain Res* 17: 205–242, 1970.